Journal of Lake and Reservoir Management 14(2-3):301-321, 1998

Development and Testing of a Nutrient-Phytoplankton Model for Cannonsville Reservoir[1]

S. M. Doerr
Upstate Freshwater Institute
P.O. Box 506
Syracuse, NY 13214

E. M. Owens
Department of Civil and Environmental Engineering
Syracuse University
Syracuse, NY 13244

R. K. Gelda
Upstate Freshwater Institute
P.O. Box 506
Syracuse, NY 13214

M. T. Auer
Department of Civil and Environmental Engineering
Michigan Technological University
Houghton, MI 49931

S. W. Effler
Upstate Freshwater Institute
P.O. Box 506
Syracuse, NY 13214

ABSTRACT

S. M. Doerr, E. M. Owens, R. K. Gelda, M. T. Auer and S. W. Effler. 1998. Development and testing of a nutrient-phytoplankton model for Cannonsville Reservoir. Lake and Reserv. Manage. 14(2-3):301-321.

A dynamic multi-layer one-dimensional mass balance nutrient-phytoplankton (eutrophication) model is developed and tested for the lacustrine zone of eutrophic Cannonsville Reservoir. The model simulates concentrations of chlorophyll (Chl), zooplankton biomass, various forms of phosphorus (P) and nitrogen (N), and dissolved oxygen (DO). Model development was integrated with, and supported by, limnological analysis of detailed monitoring data and findings of various system-specific process/kinetic studies. Model testing is supported by comprehensive monitoring data of in-reservoir concentrations and important environmental and operational forcing conditions. Model credibility is enhanced by the independent determination of a number of important model coefficients from the process/kinetic studies, which greatly constrains the role of calibration. The model performed well in simulating observations of seasonal average Chl concentration, the progressive depletions of nitrate plus nitrite from the epilimnion and DO from the hypolimnion, and the low and relatively uniform epilimnetic concentrations of other dissolved forms of N and P, and is thus an appropriate management tool to evaluate scenarios aimed at abating the reservoir's eutrophication problems.

Key Words: reservoir, eutrophication, modeling, nutrients, mass balance, model testing.

Mechanistic mass balance nutrient-phytoplankton, or eutrophication, models are quantitative frameworks that are widely used to guide management decisions for reclamation of culturally eutrophic lakes. These quantitative tools are invaluable to related research by integrating various component studies into a holistically

[1]Contribution No. 174 of the Upstate Freshwater Institute.

sound representation of an ecosystem, and to test hypotheses regarding regulating processes (e.g., Chapra 1997, Thomann and Mueller 1987). Numerous nutrient-phytoplankton models have been developed, tested, and applied (Bowie et al. 1985). Though the details of these models differ in many ways, they share certain features as they all accommodate: 1) external nutrient loading, 2) other environmental forcing conditions (e.g., light and temperature), 3) transport/mixing processes, and 4) the processes, and associated kinetics, that regulate nutrient cycling, phytoplankton growth, and phytoplankton loss processes. Nutrient-phytoplankton models are inherently more complex (i.e., more model coefficients) than most other types of water quality models (Chapra 1997, Thomann and Mueller 1987), because of the number and complexities of the nutrient cycles and phytoplankton growth and loss processes.

Establishing model credibility through testing (calibration and verification) is a fundamental step in the modeling process and is essential if these quantitative tools are to be relied upon to effectively guide related management and research efforts. Model calibration is too often constrained only by literature compilations of coefficient values used for other systems (e.g., Bowie et al. 1985). The ranges offered in these compilations are in general quite broad, and most of the listed values were derived from model calibration rather than system-specific measurement.

Here we document the development and testing of a nutrient-phytoplankton model for the lacustrine zone (Effler and Bader 1998) of Cannonsville Reservoir, NY. The goal is to simulate the seasonal distribution of chlorophyll (as a measure of phytoplankton biomass) and important forms of dissolved nutrients in response to environmental forcing conditions. The model is intended to guide management decisions to protect and improve the water quality of this reservoir as it relates to nutrient supply and phytoplankton growth and to serve as an integrator of related research studies of this system (Fig. 1). This modeling effort is rather unique in that it is supported by a number of coupled process/kinetic studies, detailed specification of environmental forcing conditions, and in-reservoir concentrations of model state variables. An important contribution of this modeling effort is the manner in which it serves to integrate the diverse research activities necessary to support the development of a credible nutrient-phytoplankton model. According to the integrated modeling approach (Fig. 1), the design of the model framework and the form of the various quantitative relationships incorporated in the model are influenced by the results of system-specific studies, rather than constraints (and potential biases) of a pre-existing framework. This integrated modeling approach results in more rigorous model testing and a more credible management and research tool by constraining the calibration process (e.g., a number of key coefficients are known, instead of being subject to the "tuning" process).

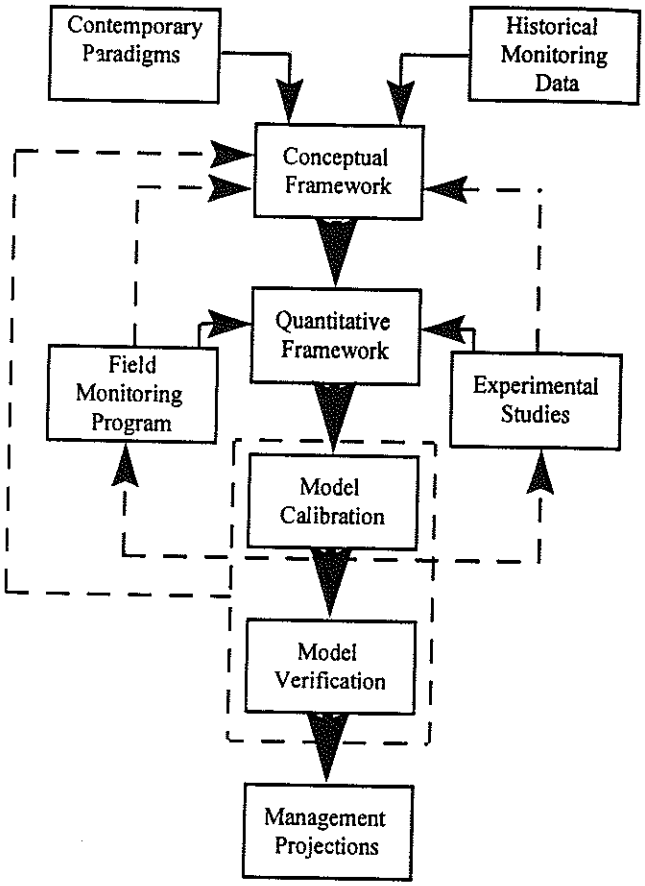

Figure 1.–The integrated modeling approach, depicting the interplay between support studies and the development and testing of a model.

Cannonsville Reservoir

General

Cannonsville Reservoir is a dimictic impoundment located in Delaware County, in upstate New York, approximately 190 km northwest of New York City (NYC). The reservoir is owned by NYC and operated by the New York City Department of Environmental Protection (NYCDEP) to supply drinking water for NYC and to augment flow in the Delaware River downstream of the reservoir. The reservoir has been in operation since 1966. Cannonsville Reservoir has a capacity of 3.73×10^8 m^3, a mean depth (when full) of

~ 19 m, and an average flushing rate of 2.6 times · y^{-1} (Owens et al. 1998).

Water leaves the reservoir by one of three pathways, flows over the spillway, withdrawals for drinking water (from a position within the lacustrine zone), and releases at the base of the dam to augment flow in the Delaware River. Drinking water can be withdrawn from depths of 10, 20 or 37 m below the spillway crest. About 80% of the water received by the reservoir is from the West Branch of the Delaware River (WBDR) (Owens et al. 1998). This inflow represents an even greater fraction of the input of critical nutrients and sediment to the reservoir.

Cannonsville Reservoir is eutrophic, manifested as high standing crops of phytoplankton, blooms of nuisance blue-green algae, low clarity, and severe depletion of oxygen in the hypolimnion (Effler and Bader 1998). Gradients in some of these trophic state indicators prevail along the longitudinal axis of the reservoir, with the least eutrophic characteristics observed in the lacustrine zone (Effler and Bader 1998). However, longitudinal (and lateral) differences within the lacustrine zone (~ 80% of the reservoir volume when it is full) are minor (Effler and Bader 1998).

Supporting Models, Monitoring Data, and Process Studies

A number of coordinated studies to support development and testing of hydrothermal (Gelda et al. 1998, Owens 1998b) and nutrient-phytoplankton models for Cannonsville Reservoir (Table 1) have been described in preceding manuscripts of this issue of the journal. The transport framework (submodel) for the one-dimensional nutrient-phytoplankton model presented here is the one-dimensional hydrothermal model (with 30 to 50 vertical layers) developed and successfully tested for the reservoir (Owens 1998c). A number of hydrodynamic and hydrothermal measurements were made (Owens 1998a,b; Table 1) in support of this model. This submodel maintains the hydrologic balance for the overall model by incorporating the budget components determined from the hydrologic model analysis of Owens et al. (1998). The relative magnitude and substantially variability of the components of the reservoir's hydrologic budget for the period of operation have been reviewed by Owens et al. (1998). The 20-m intake is used the majority of time for the water supply; the 37-m intake was used from late August to early September in 1995 because of the unusually severe drawdown (Owens et al. 1998).

External loading estimates were calculated at a time step of 1 day (Longabucco and Rafferty 1998). We have a high degree of confidence in the loads (e.g., Fig. 2a and b) because the WBDR loads were developed from a runoff event-based (e.g., according to stream hydrograph) sampling program (also included routine dry-weather sampling) that has been in place since the fall of 1991 (Longabucco and Rafferty 1998; Table 1). Substantial interannual variations in nutrient and sediment loading from WBDR have occurred (Fig. 2a and b) in response to variations in runoff (Longabucco and Rafferty 1998). Incident photosynthetically active radiation (PAR), another important forcing function for phytoplankton growth (Chapra 1997, Kirk 1994) and the seasonal heat budget (Owens 1998a,c), was measured (hourly) onsite at the dam during 1995 (Fig. 2c).

A temporally and spatially intensive monitoring program (Effler and Bader 1998) was conducted on the reservoir over the April-November interval of 1995 to support development and calibration of the hydrothermal and nutrient-phytoplankton models (Table 1). This was augmented by NYCEP's routine monitoring program that included weekly monitoring of water supply withdrawals (Effler and Bader 1998). The summer average epilimnetic concentrations of TP (23.2 $\mu g \cdot L^{-1}$) and Chl (9.6 $\mu g \cdot L^{-1}$) were both consistent with low level eutrophy. However, concentrations of particulate P (PP) and TP became largely uncoupled from Chl after May, with the drawdown of the reservoir, because of contributions of resuspended non-phytoplankton particles (e.g., tripton) (Effler et al. 1998a). Concentrations of soluble reactive P (SRP) and total ammonia ($T\text{-}NH_3$) remained very low (e.g., near detection limits) in the upper productive layers. Most of the dissolved P in these layers existed as dissolved organic P (DOP). The most conspicuous signature of phytoplankton activity imparted to a nutrient pool of the upper waters was the progressive depletion of nitrate (plus nitrite; NO_x); the NO_x concentration decreased from 700 $\mu gN \cdot L^{-1}$ in April to undetectable levels (e.g., < 10 $\mu gN \cdot L^{-1}$) in late August 1995 (Effler and Bader 1998). Filamentous cyanobacteria which are capable of nitrogen (N) fixation, dominated the phytoplankton assemblage in mid-July and remained dominant through late September (unpubl., Siegfried 1998), consistent with the reduction in the FIN ($T\text{-}NH_3 + NO_x$): TDP ratio (Effler and Bader 1998). Progressive depletion of DO from the hypolimnion, and the development of anoxia in the lowermost waters in late summer, were observed (Effler and Bader 1998). Substantial release of P from the bottom sediments was not observed during the interval of anoxia because depletion of the hypolimnetic pool of NO_x (by denitrification) was incomplete (see Effler and Bader 1998). Comparison of the hypolimnetic depletion rate of DO and the accumulation rate of SRP (soluble

reactive P) (Gächter and Mares 1985) indicated the operation of a loss process for SRP in the hypolimnion (Effler and Bader 1998).

Data available for 1994 have been selected to support verification testing for the nutrient-phytoplankton model. Certain forcing conditions differed substantially in 1994 from those of 1995; e.g., material loading and the reservoir pool size were greater in 1994 (Fig. 2a and b) (Effler and Bader 1998, Owens et al. 1998).

A number of process/kinetic studies were conducted (Table 1) to determine system-specific coefficients. Downward fluxes (units of $mg \cdot m^{-2} \cdot d^{-1}$) and settling velocities (units of $m \cdot d^{-1}$) were determined for Chl, P, N, organic carbon (C), and total suspended solids (TSS) through analyses of sediment trap collections (Effler and Brooks 1998; Table 1). The occurrence of sediment resuspension in the reservoir was documented (Effler et al. 1998a). The relative contributions of phytoplankton and non-phytoplankton particles in regulating light penetration and the availability of light to support primary production were

Table 1. –Studies and data supporting the development and testing of a one-dimensional nutrient-phytoplankton model for Cannonsville Reservoir.

Study/Data	Program Description	Reference
1. onsite meteorological measurements	wind, incident PAR, air temperature, etc. (hourly)	described by Gelda et al. 1998
2. hydrodynamic/transport processes	thermistor chains, current meters, multiple temperature profiles	Owens 1998b
3. transport submodel	development and testing	Owens 1998c
4. hydrologic budget/model	review of hydrologic budget data for period of reservoir operation; model development and testing	Owens et al. 1998
5. material loading	runoff event-based sampling of WBDR since fall 1991	Longabucco and Rafferty 1998
6. in-reservoir measurements of model state variables	program description and limnological evaluation	Effler and Bader 1998
7. downward fluxes of particulate species	sediment trap studies; calculation of settling velocities	Effler and Brooks 1998
8. sediment resuspension and associated interferences	characterization of phenomenon	Effler et al. 1998a
9. optics of reservoir	evaluation of relative roles of phytoplankton and non-phytoplankton particles in regulating light penetration	Effler et al. 1998b
10. sediment-water exchange fluxes	laboratory determinations, using sediment core samples	Erickson and Auer 1998
11. phytoplankton kinetic coefficients	laboratory experiment with the phytoplankton assemblage of the reservoir	Auer and Forrer 1998
12. bioavailability and mineralization rate of tributary PP	laboratory experiments according to DePinto et al. (1981)	Auer et al. 1998
13. zooplankton composition and and population density	analysis of weekly collections made in 1995	Siegfried 1998 (unpubl.)

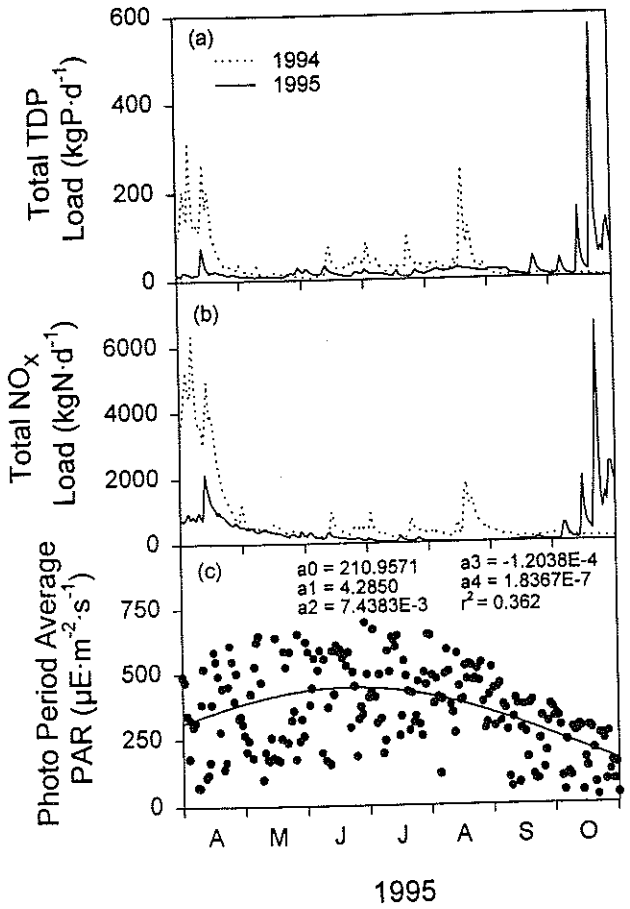

Figure 2.–Daily time series for selected forcing functions for Cannonsville Reservoir nutrient-phytoplankton model: (a) TDP loads, 1994 and 1995; (b) NO_x loads, 1994 and 1995; and (c) incident PAR for 1995, with polynomial fit of distribution.

quantified (Effler et al. 1998b; Table 1). Sediment-water exchange rates [e.g., sediment oxygen demand (SOD), P release, T-NH_3 release] were determined in laboratory microcosm studies conducted on sediment core samples, with intact sediment-water interfaces (Erickson and Auer 1998; Table 1). Phytoplankton kinetic coefficients (specific growth rate, respiration rate, light half-saturation coefficient, half-saturation coefficient for P uptake) were determined in laboratory experiments conducted with the natural phytoplankton assemblage of the reservoir (Auer and Forrer 1998; Table 1). Algal bioassays (DePinto et al. 1981) were conducted to determine the fraction of PP supplied by WBDR available to support algae growth and to determine the first order rate coefficient that describes the mineralization of PP (Auer and Forrer 1998; Table 1). Zooplankton composition and density were determined on samples collected weekly during the monitoring period of 1995 (unpubl., Siegfried 1998) to support assessments of potential phytoplankton losses from grazing.

Model Framework

Background/Approach

The nutrient-phytoplankton model for Cannonsville Reservoir has five kinetic submodels: (1) the P submodel (Fig. 3a), (2) the N submodel (Fig. 3b), (3) the Chl submodel (Fig. 3c), (4) the zooplankton submodel (Fig. 3d), and (5) the DO submodel (Fig. 3e). The kinetic expressions include the source and sink terms for each state variable, exclusive of external loading and transport-based exchange (see Appendix I).

The emphasis of this model was to accommodate and accurately quantify the important source and sink processes that are critical to effectively simulate the model's state variables (Table 2). An exception is the partitioning between available and unavailable non-living particulate P, as Auer et al. (1998) found the PP loads from WBDR contributed little to the support of phytoplankton growth. However, PP loading can enhance phytoplankton growth in the reservoir following the most extreme runoff events (Longabucco and Rafferty 1998) and may be more important in other NYC reservoirs (to be modeled in the future), so the capability has been included.

Phosphorus Submodel

Soluble reactive P is assimilated by phytoplankton, a process that is largely confined to the epilimnion of this reservoir because of limited light penetration (Effler et al. 1998b). The apparent sink for SRP in the reservoir's hypolimnion is represented as a loss to unavailable non-living PP (UNLPP) described as adsorption here (Fig. 3a), though there are other possible loss mechanisms (e.g., bacterial uptake) (Gächter and Mares 1985). Water column sources of SRP include decay (microbial) of DOP and available non-living PP (ANLPP) (Fig. 3a). Bottom sediments represent a potential source of SRP to the anoxic hypolimnion that would occur following elimination of hypolimnetic NO_x via denitrification [consistent with free energy considerations (Froelich et al. 1979)]. This recycle pathway has not been observed for the reservoir (Effler and Bader 1998, Erickson and Auer 1998) because the NO_x pool has not been completely depleted, but it is included to support simulations for scenarios of increased anthropogenic inputs (e.g., for which NO_x depletion could be complete). DOP is formed by respiration of phytoplankton and zooplankton and ineffective grazing of phytoplankton by zooplankton. Algal respiration (k_{ar}, d^{-1}) is partitioned into active

growth and maintenance (basal) according to the following expression based on the work of Laws and Chalup (1990) (Chapra 1997):

$$k_{ar} = k_b + \phi \cdot \mu \quad (1)$$

in which k_b is the basal respiration rate (d^{-1}), ϕ is the algal respiration multiplier, and μ is the specific growth rate for algae (d^{-1}). This recycle pathway is greater in the epilimnion where phytoplankton growth occurs and is diminished in the hypolimnion (e.g., $k_{ar} = k_b$) where basal respiration prevails.

Recycling of nutrients via predation losses of zooplankton (Fig. 3a) is considered insignificant. Particulate P in the form of phytoplankton and non-phytoplankton particles (ANLPP and UNLPP) settles; settling velocities of Chl (lower) and the non-living PP (higher) components were assigned according to sediment trap results (Effler and Brooks 1998; Table 1). The external loading of PP is partitioned according to the outcome of bioavailability experiments conducted on the WBDR samples (Auer et al. 1998). This load supports very little phytoplankton growth in the reservoir because the deposition rate (Effler and Brooks 1997) is greater than the rate of mineralization (Auer et al. 1998). Adjustments in kinetic rates to represent the influence of temperature in this and the other submodels are made according to the Arrhenius function

$$k_{x,T} = k_{x,20} \cdot \Theta^{T-20} \quad (2)$$

in which $k_{x,T}$ and $k_{x,20}$ are values of kinetic coefficient x at temperature T and 20 °C; and Θ is the dimensionless temperature coefficient. The exception is the linear relationship between temperature and zooplankton grazing adopted (Canale et al. 1976; Appendix I).

Resuspension is known to be a recycle pathway for particulate constituents in Cannonsville Reservoir (Effler and Brooks 1998, Effler et al. 1998a) and is represented in the conceptual frameworks of the P (Fig. 3a) and N (Fig. 3b) submodels. However, this

(a)

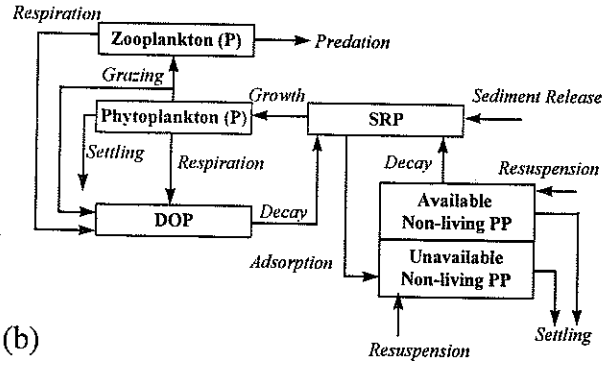

(b)

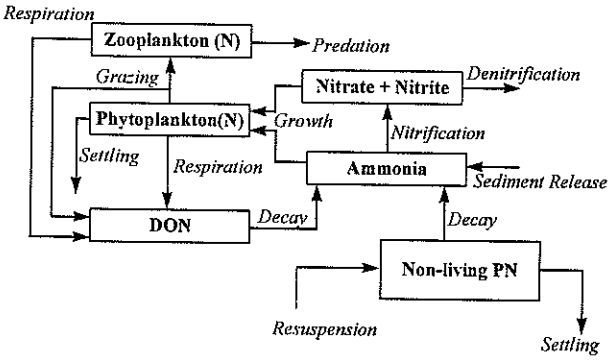

(c)

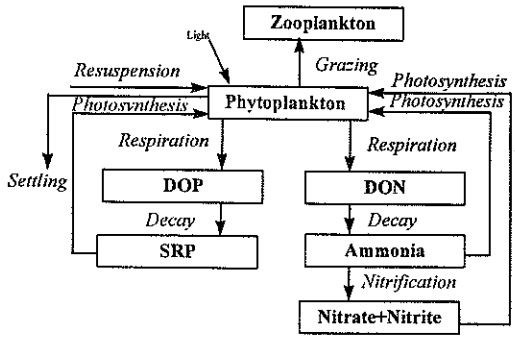

(d)

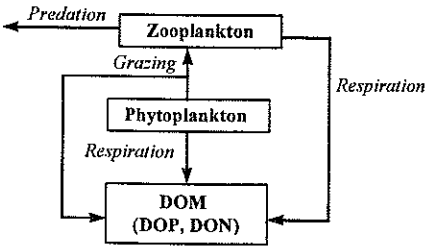

(e)

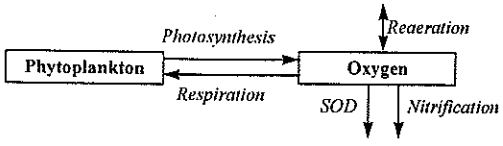

Figure 3.–Conceptual submodels for Cannonsville Reservoir nutrient-phytoplankton model: (a) phosphorus, (b) nitrogen, (c) phytoplankton, (d) zooplankton, and (e) dissolved oxygen.

Table 2.–Listing of state variables in nutrient-phytoplankton model for Cannonsville Reservoir.

Type	State Variables	Symbols*	Units
plankton	chlorophyll	Chl	$\mu g \cdot L^{-1}$
	zooplankton	Z_{DW}	$\mu g \cdot L^{-1}$
phosphorus (P)	soluble reactive P	SRP	$\mu g \cdot L^{-1}$
	dissolved organic P	DOP	$\mu g \cdot L^{-1}$
	available non-living particulate P	ANLPP	$\mu g \cdot L^{-1}$
	unavailable non-living particulate P	UNLPP	$\mu g \cdot L^{-1}$
nitrogen (N)	ammonia	$T\text{-}NH_3$	$\mu g \cdot L^{-1}$
	nitrate plus nitrite	NO_3	$\mu g \cdot L^{-1}$
	dissolved organic N	DON	$\mu g \cdot L^{-1}$
	non-living particulate N	NLPN	$\mu g \cdot L^{-1}$
other	dissolved oxygen	DO	$mg \cdot L^{-1}$
	temperature	T	°C

* e.g., see Appendix I.

process is not considered in the model testing reported here (i.e., resuspension = 0). Instead, the model is used to estimate this input and support preliminary characterization of the process.

Nitrogen Submodel

Dissolved compartments in the N submodel include $T\text{-}NH_3$, NO_x and dissolved organic N (DON); the particulate compartments include phytoplankton, zooplankton, and non-living particulate N (Fig. 3b). Either $T\text{-}NH_3$ or NO_x can be used by phytoplankton to support growth, but $T\text{-}NH_3$ is preferred for energetic reasons (Wetzel 1983). Phytoplankton in Cannonsville Reservoir draw mostly from the NO_x pool because of the low $T\text{-}NH_3$ concentrations that prevail. Nitrification (limited to T > 4.5 °C) is a loss process for $T\text{-}NH_3$ (Fig. 3b). Denitrification is a loss process for NO_x (Fig. 3b) that is operative under anoxic conditions. Both the nitrification (Cavari et al. 1977, Hall 1986) and denitrification (Seitzinger 1988) processes are assumed to operate at the sediment-water interface and were modeled according to film transfer theory (Canale et al. 1995, 1996), as described here for nitrification

$$\text{nitrification rate } (g \cdot d^{-1}) = k_{ni} \cdot A \cdot [T\text{-}NH_3] \quad (3)$$

in which k_{ni} is the film transfer nitrification coefficient ($m \cdot d^{-1}$), A is the area of sediments (m^2), and $[T\text{-}NH_3]$ is the concentration of $T\text{-}NH_3$. This is an improvement (Canale et al. 1995, 1996) over earlier models that treated these processes as first order water column phenomena (Bowie et al. 1985). Sources of $T\text{-}NH_3$ in the water column include decay of DON and non-living particulate N (NLPN) (Fig. 3b). DON is produced from respiration of phytoplankton [Eq. (1)] and zooplankton and inefficient grazing of phytoplankton by zooplankton. Particulate forms of N that settle include phytoplankton and NLPN.

Phytoplankton Submodel

Phytoplankton growth (Fig. 3c) is limited by temperature, light, and nutrient availability (Bowie et al. 1985):

$$\mu = \mu_{max} f(T) \cdot f(I) \cdot f(N) \quad (4)$$

where μ and μ_{max} are specific and maximum specific phytoplankton growth rates (d^{-1}), f(T) is the temperature factor (Arrhenius type), f(I) is the light factor, and f(N) is the nutrient factor. A Michaelis-Menton type relationship was adopted for f(I). Light extinction is partitioned according to the dynamics of Chl and the summed effect of all other attenuating components (Effler et al. 1998b). The f(N) term is described with a "minimum formulation" (Scavia 1980); only the most severely limiting nutrient (SRP or FIN) is assumed to limit growth, in contrast to a "multiplicative" representation for f(N). The "minimum formulation" is based on "Liebig's law of the minimum" which states the nutrient in shortest supply will control the growth of algae. Monod kinetics were adopted to compute f(N)

$$f(N) = \left(\frac{[s]}{K_s + [s]} \right) \quad (5)$$

in which [s] is the concentration of the limiting nutrient in the water column, and K_s is the half-saturation

constant for the limiting nutrient. This representation assumes growth rates are regulated by concentrations of nutrients external to the algae (i.e., water column) and that the nutrient composition (i.e., stoichiometry) of the algal cells remains constant. Uptake of SRP and FIN associated with phytoplankton growth (Fig. 3c) is specified by constant ratios of Chl/P and Chl/N, corresponding to the stoichiometry of the phytoplankton (Effler and Brooks 1998). The Monod representation ignores the well-documented phenomenon of luxury uptake by which nutrients are acquired and stored at levels well beyond the immediate demand for growth (Droop 1973), but luxury uptake can be ignored where the rate of change in external nutrient levels is slow relative to the rate of growth ("cellular" equilibrium) (DiToro 1980).

Loss processes for phytoplankton biomass simulated in the model include settling (specified by the sediment trap study) (Effler and Brooks 1998), respiration (specified by laboratory studies) (Auer 1998), and zooplankton grazing (estimated from zooplankton monitoring data; Fig. 3c). Respiration, excretion, and non-predatory mortality (decomposition) were lumped within the "respiration" loss process. Zooplankton grazing (a nutrient recycle pathway and sink for phytoplankton) was eliminated when (nitrogen-fixing) filamentous cyanobacteria dominated (Gliwicz and Siedlar 1980) as indicated by the FIN/TDP ratio [(26.6) (Effler and Bader 1998)].

Zooplankton and Oxygen Submodels

The herbivorous component of zooplankton has been explicitly simulated in this model, but substantial uncertainty often accompanies such predictions (Bowie et al. 1985). Inclusion of a zooplankton compartment is essential to accommodate the related watercolumn nutrient recycle pathways (Fig. 3d).

Sources of DO in the oxygen submodel include photosynthesis (largely confined to the epilimnion) and reaeration (epilimnion, only; Fig. 3e). Oxygen sinks include phytoplankton respiration, nitrification, and sediment oxygen demand (SOD; Fig. 3e). The major sink of DO in the hypolimnion is SOD. This value is specified from laboratory measurements (Erickson and Auer 1998) instead of being explicitly modeled (see Chapra 1997). Rates of microbially-mediated oxygen depletion processes decrease as DO concentrations decrease (Lam et al. 1984, Snodgrass and Ng 1985). This effect was quantified for the hypolimnion, as a multiplier (f_{OL}; dimensionless) of the depletion process, according to a Monod-type expression

$$f_{OL} = \frac{[DO]}{[DO] + K_{s,DO}} \quad (6)$$

in which $K_{s,DO}$ is the the half-saturation constant for oxygen limitation, and [DO] is the concentration of dissolved oxygen ($mg \cdot L^{-1}$).

Other Model Outputs

Outputs, other than state variables (Table 2) are calculated by the model, including downward fluxes of Chl, PP and particulate N (PN), TDP (= SRP + DOP), PP, TP (= TDP + PP), PN, TN (NO_x + T-NH_3 + DON + PN), and the FIN:TDP ratio. Time series of the simulated downward fluxes, calculated as the product of the epilimnetic concentration of particulate constituents and the settling velocity of phytoplankton (Chl; Effler and Brooks 1997), are presented for 1995 and compared to measured sediment trap fluxes. The predicted fluxes for PN and PP are associated with phytoplankton only; i.e., they do not accommodate resuspended inorganic particles that are known to have contributed to fluxes determined from trap deployments (Effler and Brooks 1998, Effler et al. 1998a). The calculated PP concentration is the sum of available and unavailable non-living PP and phytoplankton P and zooplankton P. These additional outputs have diagnostic value in analyzing model simulations.

Inputs and Modeling Protocol

The mass balance expressions of the model (Appendix I) are solved numerically using an implicit finite difference method (Owens 1998b). The time step of hydrologic, material loading, and meteorological forcing function inputs to the model is 1 day. Total loads are calculated by summing the WBDR (Longabucco and Rafferty 1998) and minor tributary loads. The minor tributary loads are estimated based on bi-weekly constituent concentrations measured at the mouth of Trout Creek (see Effler and Bader 1998; assumed representative of all minor tributaries) using loading calculation software (FLUX) developed by Walker (1987). The model computation time step is 1 hour. The model is calibrated for the April 4 to October 10 period of 1995 and verified for the May 9 to November 30 interval of 1994. The model is initialized with the observations made at the lacustrine site adjacent to the dam (Effler and Bader 1998) on the first day of measurements of each year of testing. Transport characteristics are not involved in the calibration of the water quality model. Instead these features are established independently through testing of the

Table 3.–Model coefficients independently determined to support the nutrient-phytoplankton model for Cannonsville Reservoir.

No.	Coefficient	Symbol	Value/Units	Source
1.	maximum specific growth rate for phytoplankton	μ_{max}	1.7 d^{-1}	Auer and Forrer 1998
2.	phytoplankton respiration rate	k_{ar}	0.29 d^{-1}	Auer and Forrer 1998
3.	light half saturation coefficient for phytoplankton growth	K_I	53 $\mu E \cdot m^{-2} \cdot s^{-1}$	Auer and Forrer 1998
4.	background extinction coefficient	K_W	= - 0.018xWSE†+6.67	Effler et al. 1998b
5.	multiplier for Chl component of extinction	K_c	0.02 $m^2 mg^{-1}$ Chl	Effler et al. 1998b
6.	decay coeffiicient for ANLPP mineralization	k_{pd}	0.20 d^{-1}	Auer et al. 1998
7.	sediment release rate SRP	$Rsed_{SRP,8}$	0* $mg \cdot m^{-2} \cdot d^{-1}$	Erickson and Auer 1998
8.	phosphorus half-saturation constant for phytoplankton growth	K_{SRP}	0.5 $\mu gP \cdot L^{-1}$	Auer and Forrer 1998
9.	biavailable fraction of non-living PP load	availp	25%	Auer et al. 1998
10.	Chl settling velocity	vel_{chl}	0.17 $m \cdot d^{-1}$	Effler and Brooks 1998
11.	settling velocity ANLPP and UNLPP	vel_{pp}	0.94 $m \cdot d^{-1}$	Effler and Brooks 1998
12.	settling velocity NLPN	vel_{PN}	0.46 $m \cdot d^{-1}$	Effler and Brooks 1998
13.	SOD, at 20 °C	SOD_{20}	1.06 $g \cdot m^{-2} \cdot d^{-1}$	Erickson and Auer 1998
14.	organic C to Chl ratio	a_{CChl}	80 $\mu gC \cdot \mu gChl^{-1}$	Effler and Brooks 1998
15.	organic C to N ratio of phytoplankton	a_{CN}	6.25 $\mu gC \cdot \mu gN^{-1}$	Effler and Brooks 1998

* when bottom $NO_x > 0.01$ $\mu gN \cdot L^{-1}$.
* when bottom is anoxic and $NO_x < 0.01$ $\mu gN \cdot L^{-1}$.
† WSE = water surface elevation (m).

hydrothermal model (Owens 1998c).

An unusually large number of coefficients for the nutrient-phytoplankton model were independently determined by system-specific experiments and measurements (Table 3). Other coefficients and their calibration values (Appendix I) were selected from the literature or specified according to the authors' experience on other systems. Temporal distributions of measured and simulated constituent concentrations are presented as epilimnetic and hypolimnetic volume-weighted averages, based on hypsographic data presented by Owens et al. (1998) and the measured (Effler and Bader 1988) and predicted profiles.

Model Performance

Model performance is evaluated within the context of time series of epilimnetic and hypolimnetic volume-weighted concentrations, downward fluxes (Figs. 4 to 10), and concentrations measured in the water supply

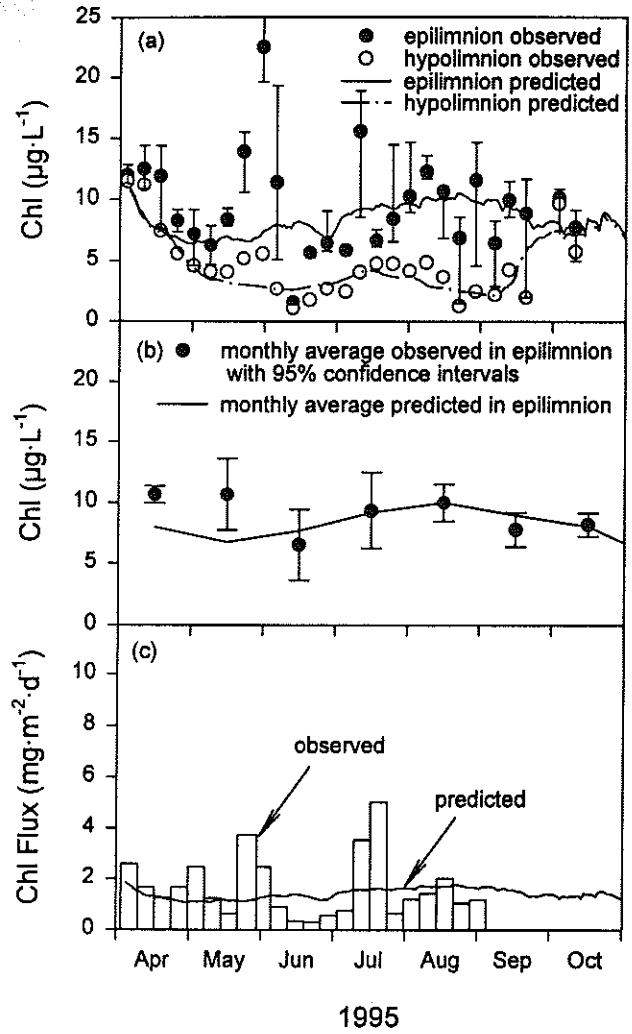

Figure 4.–Calibration testing of a nutrient-phytoplankton model for Cannonsville Reservoir: (a) Chl, vertical bars are ranges within the epilimnion, and (b) monthly average Chl, with 95% confidence limits, and (c) downward flux of Chl.

intake(s) (Fig. 11). The observations for the reservoir water column were weekly in 1995 (Figs. 4 to 7), substantially more frequent than the seasonal (e.g., monthly) resolution goal of this effort and other similar works reported in the literature. The supporting set of observations for 1994 is substantially less comprehensive with respect to frequency (bi-weekly) and parameters measured (Figs. 8 to 10). Qualitative performance criteria include the success of model simulations in matching the systematic depletions of epilimnetic NO_x and hypolimnetic DO, and the magnitudes of the Chl and dissolved nutrient pools (other than NO_x). The quantitative measure of performance was whether the monthly average model predictions fell within the bounds of ± 2 standard deviations of the observed monthly mean value for the two layers (Table 4). The standard deviation limits are based on average monthly variances for each measured state variable, as month to month differences were not statistically different. This basis of evaluation was compromised by too few observations in several instances in 1995, as well as in 1994 (Table 4).

The model performed well in simulating the primary constituents in 1995, including seasonal average Chl concentration (Fig. 4a; e.g., relative error ~ 17% for simulation period), the progressive depletion of NO_x from the epilimnion (and throughout the water column during the fall mixing period; Fig. 5a), and the progressive depletion of DO from the hypolimnion (Fig. 6; Table 4). Simulations of Chl were within the established statistical limits throughout 1995, except for the hypolimnion in May (Table 4). Predictions of NO_x for the epilimnion were within these bounds in

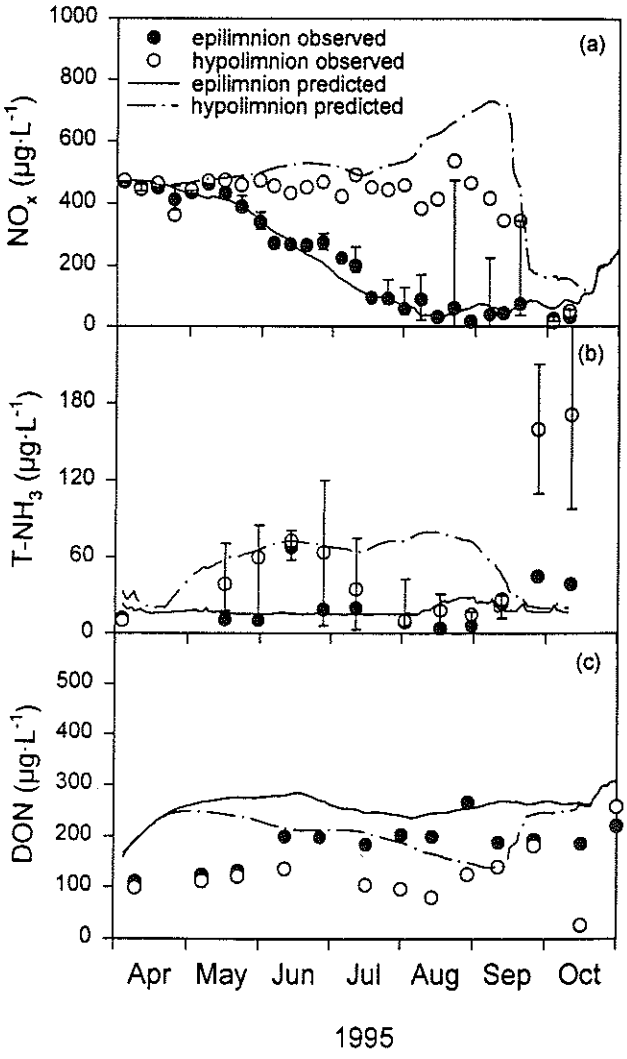

Figure 5.–Calibration testing of a nutrient-phytoplankton model for Cannonsville Reservoir: (a) NO_x, (b) $T\text{-}NH_3$, and (c) DON. Vertical bars are ranges within the layer.

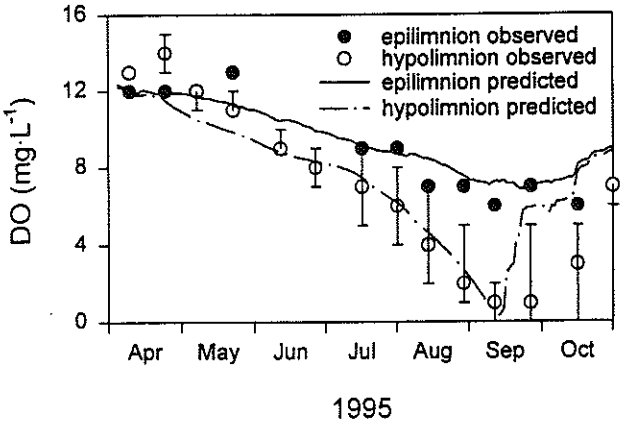

Figure 6.–Calibration testing of a nutrient-phytoplankton model for Cannonsville Reservoir, DO. Vertical bars are ranges within the hypolimnion.

5 of 7 months, and 4 of 6 months for hypolimnetic DO (Table 4). The downward flux of Chl calculated from the predictions was temporally more uniform than the observations, but the simulated cumulative flux for the April - early September interval of 1995 matched well with the cumulative flux determined from trap measurements (within 8%; Fig. 4b). These temporal short-comings in Chl deposition are at least in part a manifestation of quantifying this flux according to a single settling velocity (average of seasonal trap determinations) (Effler and Brooks 1998), though the composition of the phytoplankton changed substantially over the modeled interval (unpubl., Siegfried 1998). The model was generally successful in predicting the seasonal average epilimnetic concentrations of dissolved forms of N and P for which little seasonality was observed, including T-NH_3 (Fig. 5b), DON (Fig. 5c), and DOP (Fig. 7b). However, the modest seasonality in T-NH_3 and DON (particularly) was not well simulated (Table 4). Predicted concentrations of SRP for the epilimnion tended to be somewhat lower than the observations (Fig. 7a). These differences are not considered noteworthy at the low SRP concentrations observed (e.g., approach the detection limits of the analysis). The general seasonality in epilimnetic DO concentrations, driven largely by saturation and reaeration influences (Gelda and Auer 1996), was simulated reasonably well (Fig. 6), but there were month-to-month shortcomings in the predictions (Table 4).

Hypolimnetic concentrations of T-NH_3 (Fig. 5b), DON (Fig. 5c), SRP (Fig. 7a) and DOP (Fig. 7b) were simulated reasonably well (Table 4) in light of the limited temporal patterns observed for these constituents through the summer period. However, T-NH_3 was overpredicted from mid-July through August

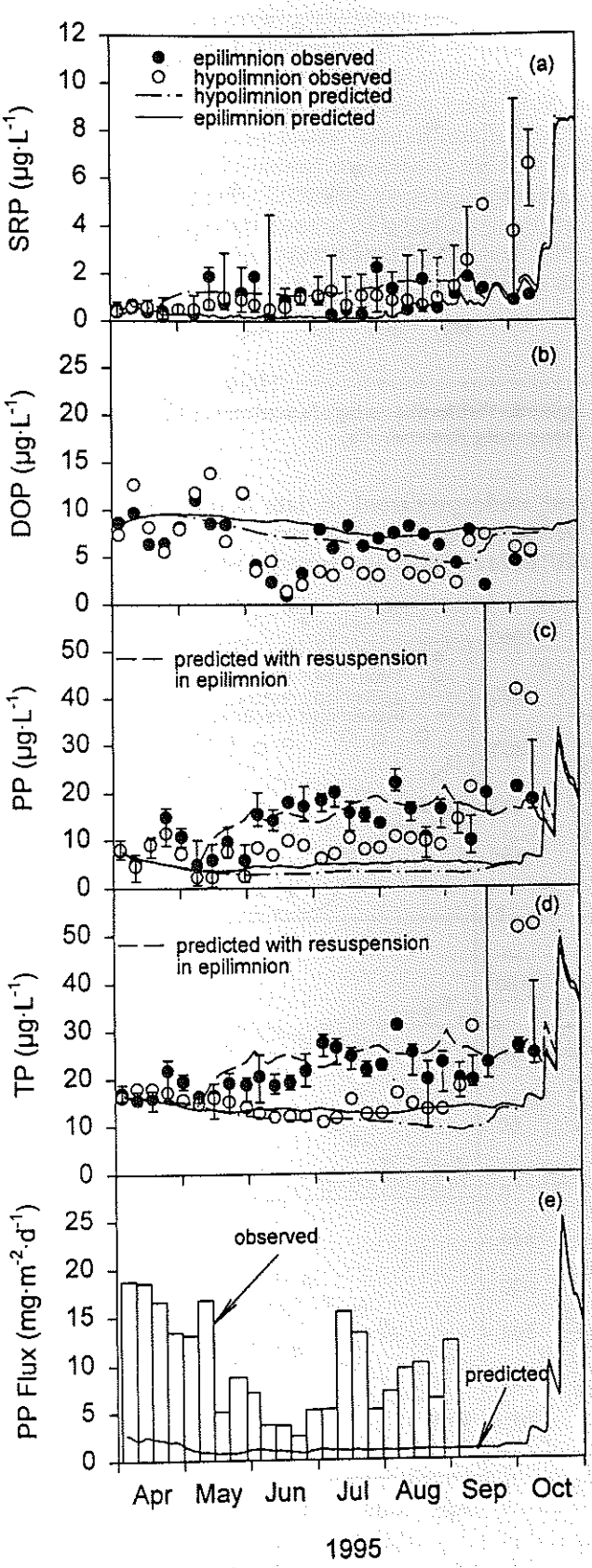

Figure 7.–Calibration testing of a nutrient-phytoplankton model for Cannonsville Reservoir: (a) SRP, (b) DOP, (c) PP, (d) TP, and (e) downward flux of PP. Vertical bars are ranges within the layer.

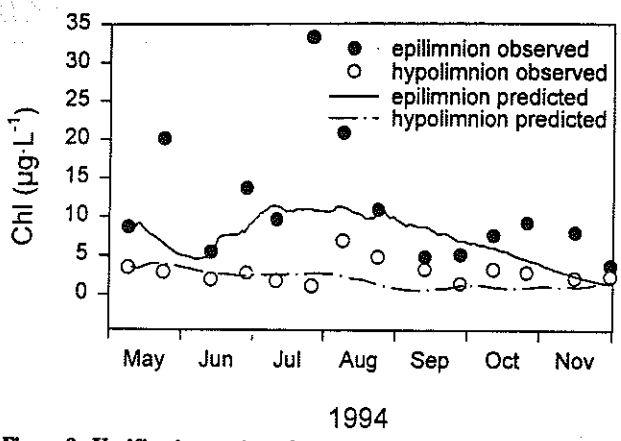

Figure 8.–Verification testing of a nutrient-phytoplankton model for Cannonsville Reservoir, Chl.

and underpredicted in late September and early October (Fig. 5b). Hypolimnetic concentrations of SRP were similarly underpredicted in the hypolimnion

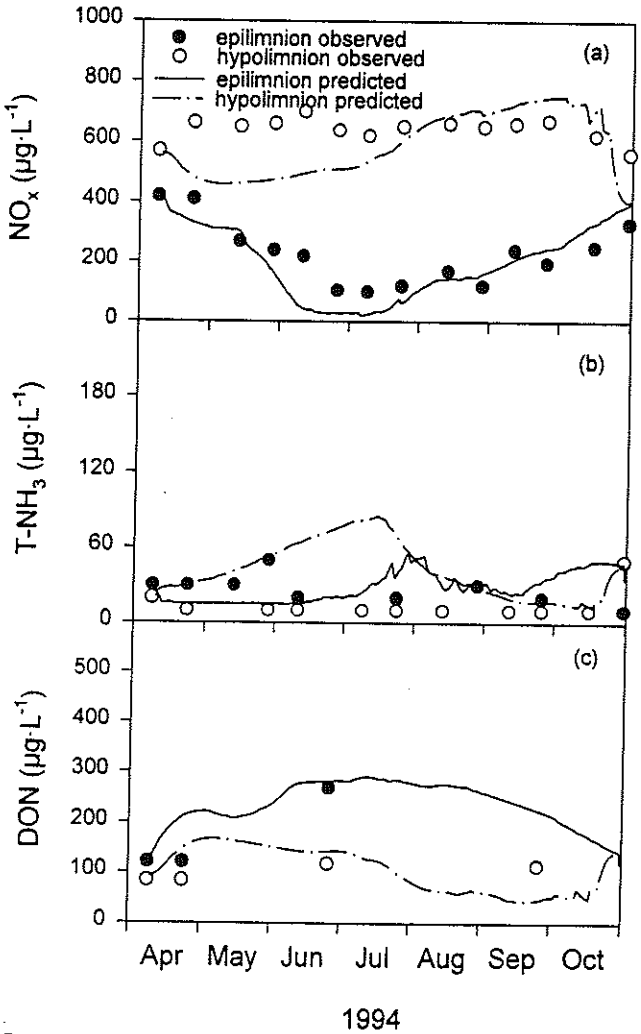

Figure 9.–Verification testing of a nutrient-phytoplankton model for Cannonsville Reservoir: (a) NO_x, (b) T-NH_3, and (c) DON.

in late September and early October (Fig. 7a). It is likely that these underpredictions of SRP and T-NH_3 during the fall mixing period are at least in part a result of not representing desorption of these constituents from resuspended sediment [indicated by the coincident increase in hypolimnetic PP (Fig. 7c), subsequently discussed] (Effler et al. 1998a). James et al. (1997) has recently explicitly modeled the distribution of ammonium N and ortho-phosphorus between dissolved and sorbed forms in Lake Okecchobee. The recovery of DO in the lower layers during the full mixing period was slower than predicted (Fig. 6; Table 4). This reflects excessive vertical mixing (Gelda and Auer 1996) in the transport submodel, a sacrifice made as part of the independent multiple-year testing of that hydrothermal model (Owens 1998c) that has affected the performance of this feature (Fig. 6) of the water quality model.

Short-term (e.g., week-to-week) variations in Chl were not well simulated, in particular, the well defined bloom (diatoms; unpubl., Siegfried 1998) of late May/early June and the subsequent abrupt decrease. Model performance, with respect to this important parameter, improves greatly when the time resolution of the weekly observations is reduced to a monthly presentation format (e.g., seasonal; Fig. 4b, Table 4), consistent with the temporal goals of most nutrient-phytoplankton models. The limitations of these models in resolving short-term variations in Chl, such as those observed in several instances in Cannonsville Reservoir in 1995 (Fig. 4a) and 1994 (Fig. 8), are widely acknowledged and explain the coarse time-averaging of observations commonly adopted in the literature. Almost certainly some of these performance problems are related to the systematic limitations of chlorophyll as a measure of phytoplankton biomass. The chlorophyll content per unit phytoplankton biomass is known to vary between species and according to ambient conditions (Kirk 1994). The chlorophyll content (e.g., ratio Chl: cellular carbon) is generally higher when the availability of nutrients is high and light is low (Chapra 1997, Laws and Chalup 1990). The peak of Chl observed in late May in 1995 appears to be qualitatively consistent with these influences; the SRP concentration was one of the highest values observed during the study (~ 2 µg · L^{-1}; Fig. 6a) at the beginning of the bloom (Fig. 4a), and light attenuation increased substantially (Effler et al. 1998b) with the increase in Chl. Chapra (1997) has developed a modeling approach to accommodate the influence of these ambient conditions on chlorophyll content of phytoplankton that depends on the incorporation of an organic carbon submodel. Canale et al. (1997) report calibration of a nutrient-organic carbon-phytoplankton model for an oligotrophic reservoir that adopts a seasonally variable Chl to cellular

carbon ratio, consistent with these interactions.

The model underpredicted concentrations of PP, particularly in the epilimnion, in 1995. Deviations became substantial in June (Fig. 7c, Table 4) when the reservoir surface started to be drawn down at a rapid rate (Effler and Bader 1998). The model failed to simulate the abrupt hypolimnetic increase in PP in September and October. Shortcomings of the same character for TP predictions (Fig. 7d) are attributable to the failure to simulate PP (compare to temporal structure of Fig. 7c). These deficiencies are a result of not representing resuspension, an important source of PP to the watercolumn of the reservoir in 1995 (Effler et al. 1998a) in the model.

The inclusion of the comparison of the predicted and observed downward fluxes of PP (Fig. 7e) is particularly instructive in this instance. The predicted flux is essentially only that component associated with phytoplankton. Thus, the great underprediction of this flux is consistent with the operation of the resuspension phenomenon and the much higher settling velocity determined for PP (mostly inorganic) compared to Chl (Effler and Brooks 1998). The model has been used (by forcing calibration) to estimate the internal load(s) of inorganic PP (UNLPP) necessary to explain the epilimnetic observations of PP. This internal load has been applied as an areal flux (mg PP · m^{-2} · d^{-1}), exerted across the 0- to 3-m depth interval (i.e., at the

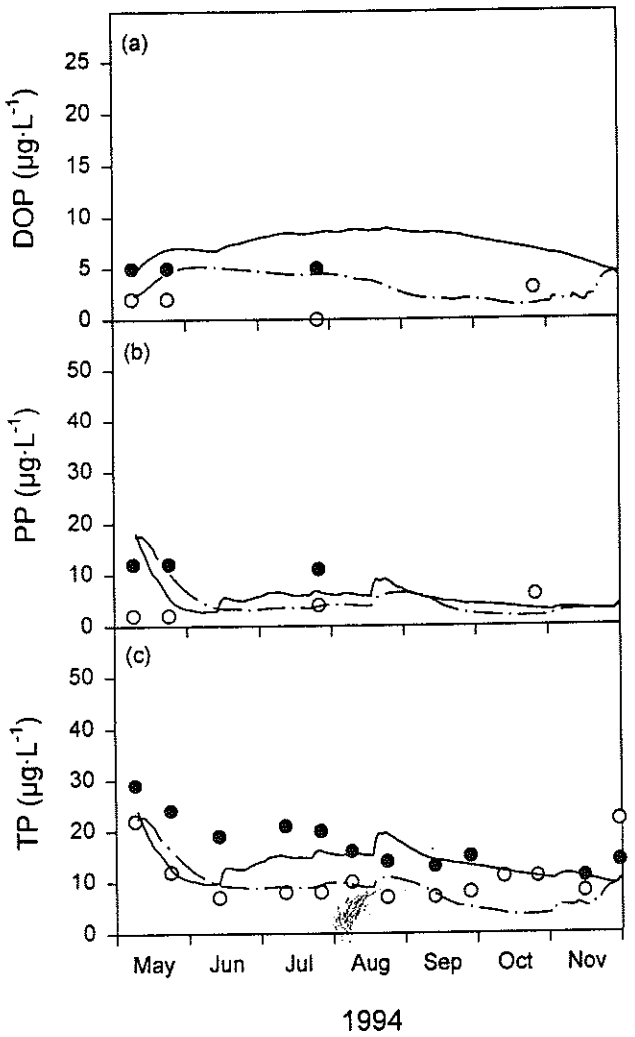

Figure 10.–Verification testing of a nutrient-phytoplankton model for Cannonsville Reservoir: (a) DOP, (b) PP, and (c) TP.

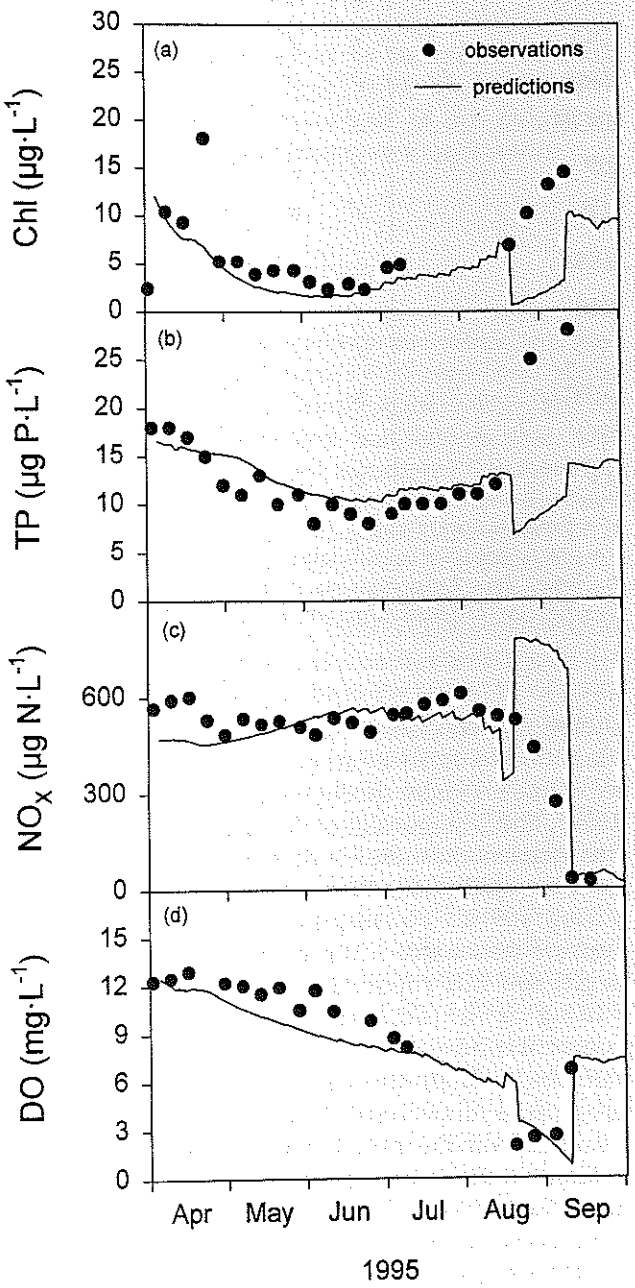

Figure 11.–Performance of nutrient-phytoplankton model for water supply withdrawal(s) of Cannonsville Reservoir, 1995: (a) Chl, (b) TP, (c) NO_x, and (d) DO.

Table 4.–Performance of nutrient-phytoplankton model for Cannonsville Reservoir; monthly simulations versus mean ± 2 std. dev., according to month and years (see footnotes and text).

Model	Epilimnion								Hypolimnion							
Variable/Yr	A	M	J	J	A	S	O	%	A	M	J	J	A	S	O	%
1995																
Chl	✓	✓	✓	✓	✓	✓	✓	100	✓	x	✓	✓	✓	✓	✓	86
NO_x	✓	✓	x	✓	✓	✓	x	71	✓	✓	x	x	x	x	x	29
T-NH_3	*	x	✓	*	x	✓	*	50	*	✓	✓	*	x	✓	*	75
DON	✓	x	x	*	✓	x	x	33	✓	x	*	*	x	✓	✓	60
DO	x	✓	x	*	✓	✓	x	50	x	✓	✓	*	✓	x	✓	67
SRP	✓	✓	✓	✓	✓	✓	x	86	✓	x	x	✓	x	✓	✓	57
DOP	✓	✓	x	✓	✓	✓	x	71	✓	✓	x	x	✓	✓	x	57
PP	✓	✓	x	x	x	✓	x	43	✓	✓	x	x	x	✓	x	43
TP	✓	x	x	x	x	x	✓	29	✓	✓	✓	✓	x	✓	x	71
1994																
Chl	✓	✓	✓	✓	x	x	✓	71	✓	✓	x	x	✓	x	x	43
NO_x	x	✓	✓	x	✓	✓	✓	71	✓	x	x	x	x	x	✓	29
T-NH_3	x	✓	*	x	✓	x	x	33	x	*	*	x	*	x	✓	25
DO	✓	✓	✓	✓	✓	✓	✓	100	✓	✓	✓	✓	✓	x	*	83
TP	x	*	x	✓	✓	x	✓	50	✓	*	x	✓	✓	x	✓	67

✓ = predictions are within observed mean ± 2 sd;
x = predictions are outside observed mean ± 2 sd;
* = fewer than 2 observations; and
% = percent of predictions within mean ± 2 sd.

shoreline), consistent with the leading mechanism identified by Effler et al. (1998a) of resuspension of shoreline sediment through wave action (see Bloesch 1994). The average value of the estimated resuspension flux, determined monthly, that resulted in a reasonable fit of the epilimnetic PP concentrations (Fig. 7c), was 4.6 $mg \cdot m^{-2} \cdot d^{-1}$. The magnitude of this estimated flux appears reasonable when compared to the average deposition flux reported for the lacustrine zone of ~ 10 $mg \cdot m^{-2} \cdot d^{-1}$ (Effler and Brooks 1998). Further, the apparent relative uniformity of the flux (coefficient of variation = 0.25) through an interval of generally progressive drawdown (Effler and Bader 1998) is consistent with the shoreline resuspension mechanism. Additional field studies, for a range of drawdown conditions, should be conducted to independently develop and test a relationship to simulate the contribution of resuspension to the reservoir's PP pool. Regardless, the existing shortcoming for this parameter does not compromise the primary goals of this modeling program, the accurate simulation of the concentrations of chlorophyll and important dissolved forms of P and N, as a function of environmental and operational forcing conditions.

Verification simulations for 1994 (i.e., same model coefficient values but different forcing conditions) were generally successful (Figs. 8 to 10), but performance was not as good as observed in 1995 (Table 4). Further, this testing was compromised because of the limited data in 1994. These limitations include the lack of sediment trap data, less frequent and vertically resolved observations, and the lack of data for some of the state variables. Simulations of Chl were rather centrally positioned within the observations (Fig. 8). The relative error for Chl for the simulation interval (~ 36%) was somewhat greater than observed for 1995 (~ 17%), and seasonal performance was not as good (Table 4). The seasonal structure of NO_x in the reservoir's epilimnion in 1994 was well simulated, including the recovery after the September minimum, though predictions were lower than the observations during the minimum (Fig. 9a). Predictions of epilimnetic

$T\text{-}NH_3$ (Fig. 9b), DON (Fig. 9c), and DOP (Fig. 10a) approximately matched the limited observations (Table 4). Hypolimnetic $T\text{-}NH_3$ was overpredicted (Fig. 9b, Table 4), as observed for late summer of 1995 (Fig. 5b). Predictions of PP (Fig. 10b) and TP (Fig. 10c) matched observations for 1994 more closely than for 1995 (Fig. 7c and d). This is consistent with the hypothesis of Effler et al. (1998a) that resuspension is coupled to the drawdown of the reservoir, as the reservoir remained more full in 1994 than in 1995 (Effler and Bader 1998). The better performance of the model for PP and TP in 1994 is expected, because less of the PP pool was resuspended sediment (i.e., relatively more of the pool was in the form of phytoplankton).

The model performed quite well in simulating the time course of concentrations of modeled constituents in the water supply intake(s) in 1995, including Chl, TP, NO_x, and DO (Fig. 11a-d). This performance further supports the credibility of the model, particularly with respect to capabilities for simulations within stratified layers and the quality of water entering the water supply. The worst performance was observed in the late August-early September interval of 1995 for Chl (Fig. 11a) and TP (Fig. 11b), when the deep intake was used [a rare occurrence (Owens et al. 1998)]. These shortcomings are consistent with the development of the benthic nepheloid layer, a manifestation of sediment resuspension (Effler et al. 1998a) that is not represented in the present framework.

Successful testing, including both calibration and verification, has been the primary basis for establishing model credibility (Chapra 1997, Thomann and Muller 1987). Widely different forcing function conditions and resulting water quality are desired for the calibration and verification cases to present a rigorous test of the capabilities of a model framework. However, the opportunity for rigorous verification testing often does not exist, or is at least compromised, because the range of conditions that prevails is often narrow. For example, the hydrologic (Owens et al. 1998) and meteorological (Gelda et al. 1998) forcing conditions encountered in 1994 and 1995 for Cannonsville Reservoir were fortuitously quite different relative to the variations encountered in the entire 30-year record. Yet the range in water quality signatures imparted and documented in these (and other) years was rather modest (Effler and Bader 1998). In such cases, the independent determination of key model coefficients through independent experiments (e.g., Auer et al. 1998, Canale et al. 1995, 1996, Doerr et al 1996, Gelda and Auer 1996) such as conducted here, serves to augment model credibility. If calibration had been achieved strictly by a "tuning" process (i.e., no system-specific studies conducted), the likelihood is great that: (1) substantially different combinations (sets) of model coefficient values could have supported calibration, and (2) shortcomings in a number of these combinations would not have emerged in verification testing. Such models cannot be considered credible as the success in hindcasting is an artifact of the compensating effects of inaccurately represented processes. The site-specific determination of a number of key coefficients enhances credibility by greatly constraining the calibration process through limiting the number of coefficients subject to "tuning". Based on the favorable performance of the Cannonsville model (Figs. 4 to 11, Table 4) and the extent to which calibration was constrained by independent determination of key coefficients (Table 3), the dissolved nutrient-phytoplankton portions of the model are supported for related management applications.

Sensitivity Analyses

Analyses were conducted with the model to establish the sensitivity of predictions of average Chl concentrations of the epilimnion for the April-October interval to uncertainty in selected coefficients that were independently determined to support this modeling effort. The sensitivity limits generally (Table 5) reflect ranges reported in the compilation of Bowie et al. (1985); i.e., are much broader than the uncertainties we have in our system-specific coefficients (e.g., Upstate Freshwater Institute 1997). Thus the sensitivity analyses depict, in part, the rather substantial uncertainties that would have been introduced in the model by selection of these coefficient values from such compilations.

Model predictions were highly sensitive to the values of the maximum specific growth rate of the phytoplankton (μ_{max}), the settling velocity of phytoplankton (vel_{Chl}), and phytoplankton respiration (k_{ar}, d^{-1}; Table 5). Predictions were somewhat less sensitive to the range of values of half-saturation constants for SRP uptake (k_{srp}) selected from the literature (Table 5). Clearly, the independent determination of these coefficients has enhanced the reliability of the nutrient-phytoplankton model for application to Cannonsville Reservoir. This finding is consistent with the position taken by other modelers (e.g., Auer and Canale 1986, Chapra 1997, Storey et al. 1993). For example, Storey et al. (1993) demonstrated with a Monte-Carlo analysis the improved credibility of model predictions of nutrient-saturated areal net phytoplankton production in Green Bay, Lake Michigan, that resulted from the use of system-specific kinetic coefficients determined on natural assemblages [similar to studies conduction on Cannonsville Reservoir (Auer and Forrer

Table 5.–Predicted average epilimnetic Chl concentrations for calibration and sensitivity simulations.

Coefficient/ Sensitivity Run	Value	Seasonal Average Chl $\mu g \cdot L^{-1}$
base case	calibration	9
μ_{max}	0.2 - 3.4 (d^{-1})	2 - 9
vel_{Chl}	0.05 - 0.6 ($m \cdot d^{-1}$)	12 - 4
K_{srp}	0.2 - 15 ($\mu g \cdot L^{-1}$)	5 - 9
k_{ar}	0.05 - 0.8 (d^{-1})	10 - 0

1998)], versus the use of literature compilations (e.g., Bowie et al. 1985). Use of literature compilations resulted in systematic differences in the best estimate of productivity, as well as much greater uncertainty in the estimate (Storey et al. 1993).

Summary/Management Implications

A dynamic one-dimensional nutrient-phytoplankton model has been developed and successfully tested for the lacustrine zone of Cannonsville Reservoir. The model simulates the seasonal concentrations of chlorophyll and dissolved species of N and P, in response to related environmental forcing conditions, including nutrient loading and reservoir operations. The model has served as an effective integrator for much of the research conducted on Cannonsville Reservoir, as presented in preceding manuscripts of this issue of the journal (Table 1). Specifically the model: (1) accommodates the forcing functions of meteorology, external nutrient and hydrologic loading, and reservoir operations (Gelda et al. 1998, Longabucco and Rafferty 1998, Owens et al. 1998), (2) utilizes the physical/transport framework of a one-dimensional hydrothermal model that has been calibrated and verified for the reservoir (Owens 1998c), (3) has been tested against comprehensive monitoring data for state variables (Effler and Bader 1998), (4) is designed to be consistent with limnological features identified from monitoring (Effler and Bader 1998) and process studies (Table 1), and (5) incorporates a number of system-specific kinetic coefficients determined from supporting studies (Table 3). The credibility of the model has been enhanced by the incorporation of system-specific values of important coefficients, thereby greatly constraining the number of coefficients subject to "tuning" in the calibration process.

The model is a potentially invaluable management tool to support evaluation of management alternatives to reduce phytoplankton growth in the reservoir and improve water quality. This model is a key component of a modeling strategy being developed to support evaluation of management options to remediate the reservoir's eutrophication problems. This strategy accommodates and reflects the impacts of a wide range of forcing conditions (~ 30 years), specified by a tested landuse/nutrient loading model (Peirson and Lounsbury 1996) and an accurate hydrologic model (Owens et al. 1998). This nutrient-phytoplankton model is now being evaluated for application to other NYC reservoirs. Further, the model is serving as a major building block in a preliminary mechanistic model for triholomethane (THM) precursors in the reservoir (see Stepczuk et al. 1997). Testing of the nutrient-phytoplankton model should continue over a number of years to evaluate performance for a range of forcing function conditions. The model should also be used to guide supporting research and to evaluate the roles of various processes in regulating primary production. In particular, efforts should be made to test and incorporate sediment resuspension, organic carbon and sediment diagenesis/water interaction submodels, partitioning of the phytoplankton community in two or more groups and accommodation of a desorption source of dissolved nutrients from resuspended sediment.

ACKNOWLEDGMENTS: This study was supported by the New York City Department of Environment Protection. This manuscript benefited from the review of Thomas James and an anonymous reviewer.

References

Auer, M. T and B. E. Forrer. 1998. Development and parameterization of a kinetic framework for modeling light- and phosphorus-limited phytoplankton growth in Cannonsville Reservoir. Lake and Reserv. Manage. 14(2-3):290-300.

Auer, M. T. and R. P. Canale. 1986. Mathematical modeling of primary production in Green Bay (Lake Michigan, USA), a phosphorus and light-limited system. Hydrobiol. Bull. 20:195-211.

Auer, M. T., K. A. Tomasoski, M. J. Babiera, M. Needham, S. W. Effler, E. M. Owens and J. M. Hansen. 1998. Particulate phosphorus bioavailability and phosphorus cycling in Cannonsville Reservoir. Lake and Reserv. Manage. 14(2-3):278-289.

Bloesch, J. 1995. Mechanisms, measurement and importance of sediment resuspension in lakes. Mar. Freshwat. Res. 46:295-304.

Bowie, G. L., W. B. Mills, D. B. Porcella, C. L. Campbell, J. R. Pagenkopf, G. L. Rupp, K. M. Johnson, P. W. H. Chan, S. A. Gherini and C. Chamberlain. 1985. Rates, constants, and kinetic formulations in surface water quality modeling, 2nd edition, EPA/600/3-85/040. U.S. Environmental Protection Agency. Athens, GA. 455 p.

Canale, R. P., S. C. Chapra, G. L. Amy and M. A. Edwards. 1997. Trihalomethane precursor model for Lake Youngs, Washington. J. Water Resour. Plan. Manage. ASCE 123:259-265..

Canale, R. P., L. M. DePalma and A. H Vogel. 1976. A plankton-based food web model for Lake Michigan. P. 33-74. *In:* R.P. Canale (Ed.) Modeling biochemical processes in aquatic ecosystems. Ann Arbor Science, Ann Arbor, MI.

Canale, R. P., R. K. Gelda and S. W. Effler. 1996. Development of testing of a nitrogen model for Onondaga Lake. Lake and Reserv. Manage. 12:151-164.

Canale, R. P., E. M. Owens, M. T. Auer and S. W. Effler. 1995. Validation of a water quality model for Seneca River, NY. J. Water Resour. Plan. Manage. ASCE 121:241-252.

Chapra, S. C. 1997. Surface water-quality modeling. McGraw-Hill, NY.

Cavari, B. Z. 1977. Nitrification potential and factors governing the rate of nitrification in Lake Kinnert. Oikos 28:285-290.

DePinto, J. V., T. C. Young and S. C. Martin. 1981. Algal-available phosphorus in suspended sediments from lower Great Lakes tributaries. J. Great Lakes Res. 7:311-325.

DiToro, D. M. 1980. Applicability of cellular equilibrium and Monod theory to phytoplankton growth kinetics. Ecol. Modeling 8:201-218.

Doerr, S. M., R. P. Canale and S. W. Effler. 1996. Development and testing of a total phosphorus model for Onondaga Lake. Lake and Reserv. Manage. 12:141-150.

Droop, M. R. 1973. Some thoughts on a nutrient limitation. J. Phycol. 9:624-638.

Effler, S. W. and A. Bader. 1998. A limnological analysis of Cannonsville Reservoir, NY. Lake and Reserv. Manage. 14(2-3):125-139.

Effler, S. W and C. M. Brooks. 1998. Gradients and dynamics in downward flux and settling velocity in Cannonsville Reservoir. Lake and Reserv. Manage. 14(2-3):213-224.

Effler, S. W., R. K. Gelda, D. L. Johnson and E. M. Owens. 1998a. Sediment resuspension in Cannonsville Reservoir. Lake and Reserv. Manage. 14(2-3):225-237.

Effler, S. W., M. G. Perkins and D. L. Johnson. 1998b. The optical water quality of Cannonsville Reservoir: spatial and temporal structures and relative role of phytoplankton and inorganic tripton. Lake and Reserv. Manage. 14(2-3):238-253.

Erickson, M. J. and M. T. Auer. 1998. Chemical exchange at the sediment-water interface in Cannonsville Reservoir. Lake and Reserv. Manage. 14(2-3):266-277.

Froelich, P. N., G. P. Klinkhammer, M. L. Bender, N. A. Luedtke, G. R. Heath, D. Cullen, P. Dauphin, D. Hammond, B. Hartman and V. Maynard. 1979. Early oxidation of organic matter in pelagic sediments of the eastern equatorial Atlantic: suboxic diagensis. Geochim. Cosmochim. Acta. 43:1075-1090.

Gächter, R. and A. Mares. 1985. Does settling seston release soluble reactive phosphorus in the hypolimnion of lakes? Limnol. Oceanogr. 30:364-371.

Gelda, R. K. and M. T. Auer. 1996. Development and testing of a dissolved oxygen model for a hypereutrophic lake. Lake and Reserv. Manage. 12(1):151-164.

Gelda, R. K., E. M. Owens and S. W. Effler. 1998. Calibration, verification, and an application of a two-dimensional hydrothermal model [CE-QUAL-W2(t)] for Cannonsville Reservoir. Lake and Reserv. Manage. 14(2-3):186-196.

Gliwicz, Z. M. and E. Siedlar. 1980. Food size limitations and algae interfering with food collection in Daphnia. Arch. Hydrobiol. 88:155-177.

Hall, G.H. 1986. Nitrification in lakes. P. 127-156. *In:* J.I. Prosser (Ed.). Nitrification. IRL Press, Washington, DC.

James, R. T., J. Martin, T. Wool and P. F. Wang. 1997. A sediment resuspension and water quality model of Lake Okeechobee. J. Amer. Water Resour. Assoc. 33:661-680.

Kirk, J. T. O. 1994. Light and photosynthesis in aquatic ecosystems. 2nd Ed. Cambridge University, London.

Lam, D. C. L., W. M. Schertzer and A. S. Fraser. 1984. Modeling the effects of sediment oxygen demand in Lake Erie water quality conditions under the influence of pollution control and weather conditions. P. 281-297. *In:* K. J. Hatcher (ed.). Sediment oxygen demand. Processes, modeling and measurement. Institute of Natural Resources, University of Georgia, Athens, GA.

Laws, E. A. and M. S. Chalup. 1990. A microbial growth model. Limnol. Oceanogr. 35:597-608.

Longabucco, P. and M. R. Rafferty. 1998. Nutrient and sediment loading to Cannonsville Reservoir from the West Branch of the Delaware River: the importance of event-based sampling. Lake and Reserv. Manage. 14(2-3):197-212.

Owens, E. M. 1998a. Thermal and heat transfer characteristics of Cannonsville Reservoir. Lake and Reserv. Manage. 14(2-3):152-161.

Owens, E. M. 1998b. Identification and analysis of hydrodynamic and transport characteristics of Cannonsville Reservoir. Lake and Reserv. Manage. 14(2-3):162-171.

Owens, E. M. 1998c. Development and testing a one-dimensional hydrothermal model for Cannonsville Reservoir. Lake and Reserv. Manage. 14(2-3):172-185.

Owens, E. M., R. K. Gelda, S. W. Effler and J. M. Hassett. 1998. Hydrologic analysis and model development for Cannonsville Reservoir. Lake and Reserv. Manage. 14(2-3):140-151.

Peirson, D. C. and D. G. Lounsbury. 1996. Application of the generalized watershed loading function (GWLF) model to the Cannonsville watershed. New York City Department of Environmental Protection, Valhalla, NY.

Scavia, D. 1980. An ecological model of Lake Ontario. Ecol. Modeling. 8:49-78.

Seitzinger, S. P. 1988. Denitrification in freshwater and coastal marine systems: ecological and geochemical significance. Limnol. Oceanogr. 33:702-724.

Snodgrass, W. J. and P. S. Ng. 1985. Biochemical models for hypolimnetic oxygen depletion in lakes impacted by wastewater discharges: 1. Alternative models. Arch. Hydrobiol./Supplement 72. 1:181-109.

Stepczuk, C. L., E. M. Owens, S. W. Effler, J. A. Bloomfield and M. T. Auer. 1998. A modeling analysis of THM precursors for a eutrophic reservoir. Lake and Reserv. Manage. 14(2-3):367-378.

Storey, M. L., M. T. Auer, A. K. Barth and J. M. Graham. 1993. Site-specific determination of kinetic coefficients for modeling algal growth. Ecol. Model. 66:181-196.

Thomann, R. V. and J. A. Mueller. 1987. Principles of surface water quality modeling and control. Harper Row, NY.

Upstate Freshwater Institute. 1997. Cannonsville Reservoir modeling project. Final report submitted to New York City Department of Environmental Protection, Valhalla, NY.

Walker, W. W. 1987. Empirical methods for predicting eutrophication in impoundments. Report 4: Phase III: Applications manual. Technical report E-81-9. U.S. Army Engineer Waterways Experimental Station, Vicksburg, MS.

Wetzel, R. G. 1983. Limnology, 2nd ed. Saunders College, Philadelphia, PA.

APPENDIX I

Mass Balance Equations

Plankton Sub-Models

Chl

$$\frac{dChl_i}{dt} = \mu_i \cdot Chl_i - k_{ar,i} \cdot Chl_i \cdot f_{OL,i} - C_{g,i} \cdot Z_{DW,i} \cdot Chl_i + \frac{vel_{Chl} \cdot A_{i+1} \cdot Chl_{i+1}}{V_i} - \frac{vel_{Chl} \cdot A_{i+1} \cdot Chl_i}{V_i} + S_R$$

where

Chl_i = chlorophyll in layer i, $\mu gChl \cdot L^{-1}$;

i = current model layer, ($\cong$1 - 50);

dt = time step, day;

μ_i = specific growth rate for phytoplankton in layer i, $\mu_i = \mu_{max} \cdot f(N)_i \cdot f(T)_i \cdot f(I)_i$, d^{-1};

μ_{max} = maximum specific growth rate for phytoplankton, 1.7 d^{-1};

$f(N)_i$ = phytoplankton growth nutrient limitation term in layer i, $f(N)_i$ = min{$f(SRP)_i$, $f(IN)_i$}, dimensionless;

$f(SRP)_i$ = phosphorus limitation term for phytoplankton growth in layer i,

$$f(SRP)_i = \frac{SRP_i}{K_{SRP} + SRP_i}, \text{ dimensionless;}$$

K_{SRP} = phosphorus half saturation constant, 0.5 $\mu gP \cdot L^{-1}$;

SRP_i = soluble reactive phosphorus in layer i, $\mu gP \cdot L^{-1}$;

$f(IN)_i$ = inorganic nitrogen limitation term for phytoplankton growth in layer i,

$$f(IN)_i = \frac{IN_i}{K_{IN} + IN_i}, \text{ dimensionless;}$$

K_{IN} = inorganic nitrogen half saturation constant, 0.1 $\mu gN \cdot L^{-1}$;

IN_i = inorganic nitrogen in layer i, $IN_i = NO_{X,i} + T\text{-}NH_{3,i}$;

$NO_{X,i}$ = sum of nitrate plus nitrite in layer i, $NO_{X,i} = NO_{2i} + NO_{3,i}$, $\mu gN \cdot L^{-1}$;

$T\text{-}NH_{3,i}$ = total ammonia in layer i, $\mu gN \cdot L^{-1}$;

$f(T)_i$ = temperature correction coefficient for phytoplankton growth in layer i, $f(T)_i = \theta_{\mu}^{(Ti-20)}$, dimensionless;

T_i = temperature of layer i, °C (Owens 1997b);

θ_{μ} = temperature correction coefficient for phytoplankton growth, 1.03 dimensionless;

$f(I)_i$ = light limitation term for phytoplankton growth in layer i,

$$f(I)_i = \frac{par_i}{K_I + par_i}, \text{ dimensionless;}$$

par_i = daily average photosynthetically active radiation at layer in layer i, $par_i = par_o \cdot e^{-kd,i \cdot zi}$, $\mu E \cdot m^{-2} \cdot d^{-1}$;

par_o = daily average photosynthetically active radiation at the surface of the reservoir, forcing function input daily, $\mu E \cdot m^{-2} \cdot d^{-1}$;

$k_{d,i}$ = light extinction coefficient at layer i, $k_{d,i} = K_C \cdot CHL_i + K_W$, m^{-1};

K_C = chlorophyll multiplier, 0.02 $L \cdot \mu gChl^{-1} \cdot m^{-1}$;

K_W = background extinction, 0.55 m^{-1};

z_i = the depth of layer i, m;

K_I = light half saturation constant, 53 $\mu E \cdot m^{-2} \cdot d^{-1}$;

$k_{ar,i}$ = phytoplankton respiration coefficient in layer i, $K_{ar,i} = k_{b,i} \cdot + \phi \cdot \mu_i$, 0.29 d^{-1};

$k_{b,i}$ = basal respiration rate in layer i, $k_{b,i} = k_{b,20} \cdot \theta_{ar}^{(Ti-20)}$, d^{-1};

$k_{b,20}$ = 0.06 d^{-1};

θ_{ar} = temperature correction coefficient for phytoplankton respiration, 1.03 dimensionless;

ϕ = phytoplankton growth-related respiration multiplier, 0.135 dimensionless;

$f_{OL,i}$ = rate multiplier for respiratory processes in layer i,

$$f_{OL,i} = \frac{DO_i}{DO_i + K_{s,DO}}, \text{ dimensionless;}$$

DO_i = dissolved oxygen in layer i, $mg \cdot L^{-1}$;

$K_{s,DO}$ = half saturation constant, 0.1 $mg \cdot L^{-1}$;

$C_{g,i}$ = zooplankton filtering rate (grazing rate) in layer i,

$$C_{g,i} = C_{g,20} \cdot \frac{T_i}{20}, \text{ } L \cdot mgDW^{-1} \cdot d^{-1};$$

$C_{g,20}$ = 1.0 $L \cdot mgDW^{-1} \cdot d^{-1}$;

$Z_{DW,i}$ = zooplankton dry weight in layer i, $\mu gDW \cdot L^{-1}$;

vel_{Chl} = settling velocity of chlorophyll, $0.17\ m \cdot d^{-1}$;

A_i = area current layer i, m^2;

A_{i+1} = area of i+1 layer, m^2;

S_R = internal source due to resuspension

= $K_{Res,Chl}(E_{critical}-E_i)$ if $E_{WS}<E_{critical}$ and $E_i<E_{critical}$

= 0, otherwise $K_{Res,Chl}$ = empirical constant for resuspension of phytoplankton, $mg \cdot m^{-3} \cdot d^{-1}$;

E_i = elevation of layer i, m;

E_{WS} = water surface elevation, m and,

$E_{critical}$ = critical water surface elevation at which resuspension begins, m.

Z_{DW}

$$\frac{dZ_{DW,i}}{dt} = C_{g,i} \cdot Z_{DW,i} \cdot Chl_i \cdot eff \cdot \left[\frac{a_{ZP}}{a_{CHLP}}\right] - k_{zr,i} \cdot Z_{DW,i} \cdot f_{OL,i} - k_{zp} \cdot Z_{DW,i} \cdot f_{OL,i}$$

where

eff = zooplankton grazing efficiency, 0.6 dimensionless;

a_{ZP} = zooplankton dry weight to phosphorus ratio, $0.089\ mgDW \cdot \mu gP^{-1}$;

a_{CHLP} = chlorophyll to phytoplankton particulate phosphorus, $2.0\ \mu gChl \cdot \mu gP^{-1}$;

$k_{zr,i}$ = zooplankton respiration rate in layer i, $k_{zr,i} = k_{zr,20} \cdot \theta_{zr}^{(Ti-10)}$, d^{-1};

$k_{zr,20}$ = $0.089\ d^{-1}$;

θ_{zr} = temperature correction coefficient for zooplankton respiration, 1.08 dimensionless and,

k_{zp} = zooplankton predation rate, $0.045\ d^{-1}$.

Phosphorus Sub-Model

SRP

$$\frac{dSRP_i}{dt} = -\mu_i \cdot \frac{Chl_i}{a_{CHLP}} + k_{op,i} \cdot DOP_i \cdot f_{OL,i} + k_{pd,i} \cdot ANLPP_i \cdot f_{OL,i} - k_{ad} \cdot SRP_i + \frac{Rsed_{SRP,i} \cdot A}{V_i}$$

where

$k_{op,i}$ = dissolved organic phosphorus decay rate constant in layer i, $k_{op,i} = k_{op,20} \cdot \theta_{od}^{(Ti-20)}$, d^{-1};

$k_{op,20}$ = $0.05\ d^{-1}$;

θ_{od} = temperature correction coefficient of dissolved organic phosphorus and nitrogen decay , 1.08, dimensionless;

DOP_i = dissolve organic phosphorus in layer i, $\mu gP \cdot L^{-1}$;

$k_{pd,i}$ = available non-living particulate phosphorus decay in layer i, $k_{pd,i} = k_{pd,20} \cdot \theta_{dpn}^{(Ti-20)}\ d^{-1}$;

$k_{pd,20}$ = $0.06\ d^{-1}$;

θ_{dpn} = temperature correction coefficient for available non-living particulate phosphorus and non-living particulate nitrogen decay, 1.08 dimensionless;

$ANLPP_i$ = available non-living particulate phosphorus in layer i, $\mu gP \cdot L^{-1}$;

k_{ad} = adsorption of SRP to UNAPP (in hypolimnion), $0.1\ d^{-1}$;

$Rsed_{SRP,i}$ = soluble reactive phosphorus sediment release, $Rsed_{SRP,i} = Rsed_{SRP,8} \cdot \theta_{SED}^{(Ti-8)} = 0$, $mgP \cdot m^{-2} \cdot d^{-1}$;

$Rsed_{SRP,8}$ = if $DO_{X,i} > 10 \mu g \cdot L^{-1}$ and $NO_{X,i} \geq 0.01$ then $Rsed_{SRP,8} = 0$, if $DO_{X,i} < 10$ and $NO_{X,i} \leq 0.01$ then $Rsed_{SRP,8} = 12.9\ mgP \cdot m^{-2} \cdot d^{-1}$;

θ_{SED} = temperature correction coefficient for phosphorus and nitrogen release, 1.06 dimensionless;

V_i = the volume of layer i, m^3 and,

A = sediment area, $A = A_{i+1} - A_i$, m^2.

DOP

$$\frac{dDOP_i}{dt} = \frac{k_{zr,i} \cdot Z_{DW,i} \cdot f_{OL,i}}{a_{ZP}} + \frac{C_{g,i} \cdot Z_{DW,i} \cdot Chl_i \cdot (1\text{-}eff)}{a_{CHLP}} + \frac{k_{ar,i} \cdot Chl_i \cdot f_{OL,i}}{a_{CHLP}} - k_{op,i} \cdot DOP_i \cdot f_{OL,i}$$

ANLPP

$$\frac{dANLPP_i}{dt} = -k_{pd,i} \cdot ANLPP_i \cdot f_{OL,i} + \frac{vel_{pp} \cdot A_{i+1} \cdot ANLPP_{i+1}}{V_i} - \frac{vel_{pp} \cdot A_{i+1} \cdot ANLPP_i}{V_i} + S_R$$

where

vel_{pp} = settling of available and unavailable and unavailable non-living particulate phosphorus, 0.94 m · d^{-1}, and

S_R = internal source due to resuspension

= $K_{Res,ANLPP}$ ($E_{critical}$-E_i) if E_{WS}<$E_{critical}$ and E_i<$E_{critical}$

= 0, otherwise $K_{Res,ANLPP}$ = empirical constant for resuspension of ANLPP, mg · m^{-3} · d^{-1}.

UNLPP

$$\frac{dUNLPP_i}{dt} = K_{ad} \cdot SRP_i + \frac{vel_{pp} \cdot A_{i+1} \cdot UNLPP_{i+1}}{V_i} - \frac{vel_{pp} \cdot A_{i+1} \cdot UNLPP_i}{V_i} + S_R$$

where

$UNLPP_i$ = unavailable non-living particulate phosphorus in layer i, µgP · L^{-1} and,

S_R = internal source due to resuspension

= $K_{Res,UNLPP}$ ($E_{critical}$-E_i) if E_{WS}<$E_{critical}$ and E_i<$E_{critical}$

= 0, otherwise $K_{Res,UNLPP}$ = empirical constant for resuspension of UNLPP, mg · m^{-3} · d^{-1}.

Nitrogen Sub-Model

T-NH $_{3,i}$

$$\frac{dT-NH_{3,i}}{dt} = k_{on,i} \cdot DON_i \cdot f_{OL,i} - \mu_i \cdot \frac{Chl_i \cdot pref_{T\text{-}NH3,i}}{a_{CHLN}} + k_{nd,i} \cdot NLPN_i \cdot f_{OL,i} + \frac{Rsed_{T\text{-}NH3,i} \cdot A}{V_i} - \frac{k_{ni,i} \cdot T-NH_{3,i} \cdot f_{OL,i} \cdot A}{V_i}$$

where

$k_{on,i}$ = dissolved organic nitrogen decay, $k_{on,i}$ = $k_{on,20} \cdot \theta_{od}^{(Ti-20)}$, d^{-1};

$k_{on,20}$ = 0.05 d^{-1};

DON_i = dissolved organic nitrogen in layer i, µgN · L^{-1};

$pref_{T\text{-}NH3,i}$ = ammonia preference by phytoplankton, if T-$NH_{3,i}$ >10 then $pref_{T\text{-}NH3,i}$ = 1, if T-$NH_{3,i}$ <10 then $pref_{T\text{-}NH3,i}$ = 0, dimensionless;

a_{CHLN} = chlorophyll to nitrogen ratio, 0.069 µgChl · µgN^{-1};

$k_{nd,i}$ = non-living particulate nitrogen decay in layer i, $k_{nd,i}$ = $k_{nd,20} \cdot \theta_{dpn}^{(Ti-20)}$, d^{-1};

$k_{nd,20}$ = 0.15 d^{-1};

$NLPN_i$ = non-living particulate nitrogen in layer i, µgN · L^{-1};

$Rsed_{T\text{-}NH3,i}$ = total ammonia sediment release in layer i, $Rsed_{T\text{-}NH3,i}$ = $Rsed_{T\text{-}NH3,8} \cdot \theta_{SED}^{(Ti-8)}$, mgN · m^{-2} · d^{-1};

$Rsed_{T\text{-}NH3,8}$ = 0.0 mgN · m^{-2} · d^{-1};

$k_{ni,i}$ = nitrification rate, if then $k_{ni,i}$ = $k_{ni,20} \cdot \theta_{ni}^{(Ti-20)}$, m · d^{-1};

$k_{ni,20}$ = T_i < 4.5°C then $k_{ni,20}$ = 0, if T_i > 4.5°C $k_{ni,20}$ = 1.2 m · d^{-1}, and,

θ_{ni} = temperature correction coefficient for nitrification, 1.05 dimensionless.

NO_X

$$\frac{dNO_{X,i}}{dt} = -\mu_i \cdot \frac{Chl_i \cdot pref_{NOX,i}}{a_{CHLN}} - \frac{k_{deni,i} \cdot NO_{X,i} \cdot A}{V_i} + \frac{k_{ni,i} \cdot T\text{-}NH_{3,i} \cdot f_{OL,i} \cdot A}{V_i}$$

where

$pref_{NOX,i}$ = nitrate preference by phytoplankton, if T-$NH_{3,i}$ >10 then $pref_{NOX,i}$ = 0, if T-$NH_{3,i}$ <10 then $pref_{NOX,i}$ = 1, dimensionless;

$k_{deni,i}$ = denitrification rate in layer i, $k_{deni,i}$ = $k_{deni,20} \cdot \theta_{deni}^{(Ti-20)}$ m · d^{-1};

$k_{deni,20}$ = if DO_i >10µg · L^{-1} then $k_{deni,20}$ = 0, if DO_i <10µg · L^{-1} then $k_{deni,20}$ = 0.4 m · d^{-1}, and

θ_{deni} = temperature correction coefficient for denitrification, 1.06 dimensionless.

DON

$$\frac{dDON_i}{dt} = \frac{k_{ar,i} \cdot Z_{DW,i} \cdot f_{OL,i}}{a_{ZN}} + \frac{C_{g,i} \cdot Z_{DW,i} \cdot Chl_i \cdot (1-eff)}{a_{CHLN}} + \frac{k_{ar,i} \cdot Chl_i \cdot f_{OL,i}}{a_{CHLN}} - k_{on,i} \cdot DON_i \cdot f_{OL,i}$$

where

a_{ZN} = zooplankton to nitrogen ratio, 0.0102 mgDW · μgN^{-1}.

NLPN

$$\frac{dNLPN_i}{dt} = -k_{nd} \cdot NLPN_i \cdot fol_i + \frac{vel_{PN} \cdot A_{i+1} \cdot NLPN_{i+1}}{V_i} - \frac{vel_{PN} \cdot A_{i+1} \cdot NLPN_i}{V_i} + S_R$$

where

vel_{PN} = settling velocity of particulate nitrogen, 0.46 m · d^{-1}, and

S_R = internal source due to resuspension

= $K_{Res,NLPN}$ ($E_{critical}$-E_i) if E_{WS}<$E_{critical}$ and E_i<$E_{critical}$

= 0, otherwise $K_{Res,NLPN}$= empirical constant for resuspension of NLPN, mg · m^{-3} · d^{-1}.

Dissolved Oxygen Sub-Model

DO

$$\frac{dDO_i}{dt} = k_L(DO_{sat} - DO_s)\frac{A_s}{V_s} + (\mu_i - k_{ar}) \cdot Chl_i \cdot a_{OC} \cdot a_{CCHL} \cdot f_{OL,i} - k_{nd} \cdot NLPN_i \cdot a_{CN} \cdot a_{OC} \cdot f_{OL,i} - k_{pd} \cdot ANLPP_i \cdot a_{CP} \cdot a_{OC} \cdot f_{OL,i} - k_{ni,i} \cdot T - NH_{3,i} \cdot \frac{A}{V_i} \cdot a_{ON} \cdot f_{OL,i} - \frac{SOD_i \cdot f_{OL,i} \cdot A}{V_i}$$

where

a_{OC} = oxygen to carbon ratio, 2.67 μgO · μgC^{-1};

a_{CCHL} = carbon to chlorophyll ratio, 80.0 μgC · μgChl^{-1};

a_{CN} = carbon to nitrogen ratio, 6.25 μgC · μgN^{-1};

a_{CP} = carbon to phosphorus ratio, 21.85 μgC · μgP^{-1};

a_{ON} = oxygen to nitrogen ratio, 4.57 μgO · μgN^{-1};

SOD_i = sediment oxygen demand in layer i, SOD_i = $SOD_i \cdot \theta_{SOD}^{(Ti-20)}$;

SOD_{20} = 1.06 g · m^{-2} · d^{-1};

θ_{SOD} = temperature correction coefficient for sediment oxygen demand, 1.065 dimensionless;

$k_{L,20}$ = reaeration coefficient at 20°C, m/d

= 0.057 U^2 for U>3.5 m/s

= 0.2 U for U<3.5 m/s;

$k_{L,T}$ = $k_{L,20}\,\theta_{Reaer}^{(T-20)}$;

U = wind velocity (m/s);

θ_{Reaer} = temperature correction coefficient for reaeration, 1.24 dimensionless;

DO_{sat} = saturation DO concentration, μg · L^{-1};

DOs = DO in surface layer, μg · L^{-1};

A_S = Area of surface layer, m^2, and

V_S = Volume of surface layer, m^3.